Journal of the Air & Waste Management Association
Publication details, including instructions for authors and subscription information:
http://www.tandfonline.com/loi/uawm20

A Two-Reservoir Model to Simulate the Air Discharged from a Pulse-Jet Cleaning System

Wu-Shung Fu [a] & Jia-Shyan Ger [a]
[a] Department of Mechanical Engineering , National Chiao Tung University , Taiwan , Republic of China
Published online: 27 Dec 2011.

To cite this article: Wu-Shung Fu & Jia-Shyan Ger (1999) A Two-Reservoir Model to Simulate the Air Discharged from a Pulse-Jet Cleaning System, Journal of the Air & Waste Management Association, 49:8, 894-905, DOI: 10.1080/10473289.1999.10463865

To link to this article: http://dx.doi.org/10.1080/10473289.1999.10463865

TECHNICAL PAPER

ISSN 1047-3289 *J. Air & Waste Manage. Assoc.* **49**:894-905

A Two-Reservoir Model to Simulate the Air Discharged from a Pulse-Jet Cleaning System

Wu-Shung Fu
Department of Mechanical Engineering, National Chiao Tung University, Taiwan, Republic of China

Jia-Shyan Ger
Department of Mechanical Engineering, National Chiao Tung University, Taiwan, Republic of China

ABSTRACT

This work presents a novel two-reservoir model to simulate, for a pulse-jet cleaning system, the air discharged from an air reservoir via a diaphragm valve to a blowpipe and ultimately into the atmosphere. The air reservoir and blowpipe are referred to reservoir 1 and reservoir 2, respectively. The proposed model consists of (1) a set of governing equations that are solved by a finite difference and (2) an iterative calculation method to describe the physical phenomena. The feasibility of the proposed model is also evaluated via experiments performed herein. Comparing the mass flow rates predicted by the proposed model with those of the benchmark solutions reveals that the model predictions are about 10% overestimated. In addition, the proposed model is more accurately simulated by considering the friction effects induced by the exit of the air reservoir and the nozzles on the blowpipe. The former increases the Mach number of the air and equals that of a frictional pipe of $4fLe/D_h$. The latter decreases the mass flow rate discharged from the nozzles. A discharge coefficient Cd_n is introduced to represent the ratio of the mass flow rate discharged from a real nozzle and an ideal one. Moreover, experimental methods are developed to determine the values of $4fLe/D_h$ and Cd_n. When the parameters of $4fLe/D_h$ and Cd_n were included in the model, the accuracy of the model predictions was significantly improved. The deviations between the mass flow rates of the model predictions and the bench mark solutions were markedly reduced to 3%.

IMPLICATIONS

Pulse-jet cleaning systems have found extensive industrial use in removing dust cakes on surfaces of filter media. This study presents a novel means of accurately predicting mass-flow rate and pressure, which play important roles in the cleaning efficiency of a pulse-jet cleaning system. Employing the proposed model allows us to realize how the cleaning parameters of a pulse-jet cleaning system affect the air pulse discharged from the nozzles on the blowpipe. This model facilitates the design and operation of a pulse-jet cleaning system.

INTRODUCTION

Due to the high efficiency of dust collection, bag filters with pulse-jet cleaning have found many industrial applications for separation of fine dust from dust-laden gas stream. The mechanisms of a pulse-jet cleaning system have been investigated in many studies.[1-5]

In a related study, Morris[1] examined the relationship between the air usage of a jet nozzle with various sizes and the energy usage for a pulse-jet cleaning process. Results of that study indicated that the energy usage is independent of the size of jet nozzle. In addition, a larger-diameter jet nozzle implies a larger volume of the used air with a lower pressure. Bouilliez[2] indicated that the most important cleaning factors are the reverse gas-flow capacity induced in the filter element and the duration of the reverse gas flow, which must be sufficiently large and long enough to inflate the bag completely. Sievert and Löffler[3] investigated how various pulse-jet cleaning system parameters influence the pressure pulse in a pulse-jet filter. According to their results, reservoir pressure, valve geometry, pulse duration, blowpipe diameter, and discharge nozzle diameter markedly affect the cleaning performance. Ravin and Humphries[4] investigated the factors influencing the cleaning effectiveness and power consumption of pulse-jet filters. Their results suggested that the cleaning effectiveness appears to depend on magnitude of the fabric deceleration, pressure of the air reservoir, and size of the jet nozzle. Hajek and Peukert[5] investigated the cleaning efficiency of ceramic high-temperature filter, indicating that the increment of a number of jet nozzles of a blowpipe under a finite reservoir volume caused a decrease in both the initial pressure peak and the reverse

flow period. In addition, a decrease in the reverse flow period implied a significant decrease in the cleaning efficiency. From their results, they concluded that a well-designed cleaning system must produce a sufficiently high pulse pressure and must allow adequate time for the dust sedimentation.

The above investigations confirm that the cleaning performance of a pulse-jet cleaning system is largely affected by cleaning parameters such as volume of the air reservoir, air pressure in the air reservoir, valve flow coefficient of the diaphragm valve, size of the blowpipe, and diameter and number of jet nozzles on the blowpipe. As the cleaning process is executed, the compressed air discharges instantaneously from the air reservoir via the diaphragm valve into the blowpipe and increases the pressure of the air in the blowpipe. The pressurized blowpipe then jets the high pressure air through the numerous nozzles drilled on the blowpipe into the corresponding bag filters. The high pressure air not only inflates the bag filter abruptly, but it also penetrates from the inner to the outer surfaces of the bag filter. By doing so, the dust deposited on the outer surface of the bag filter can be effectively removed. From the above processes, we can infer that the properties of the air discharged from the blowpipe profoundly influence cleaning efficiency. The air filling up and discharged from the blowpipe, however, is heavily affected by the following parameters: volume and pressure of the reservoir, flow characteristics of the diaphragm valve, size of the blowpipe, and size and number of the jet nozzles on the blowpipe. This complicates the theoretical or experimental analysis of the above process. Consequently, relatively few attempts have been made to develop an approximate model to simulate the above process.

Our recent investigation proposed a concise method to determine valve flow characteristics.[6] In this study, we utilized the determined flow characteristics of the diaphragm valve to investigate the process of the high-pressure air filling up and discharged from the blowpipe. A two-reservoir model is proposed to predict the air properties of air in the air reservoir and blowpipe during the cleaning process. The air reservoir and blowpipe are referred to reservoir 1 and reservoir 2, respectively. The proposed model consists of (1) a set of governing equations that are solved by a finite difference and (2) an iterative calculation method to describe the physical phenomena. In addition, four pressure transmitters were used to measure the pressure variations of the air at various locations during the process. The measured pressure variations of the air in the reservoir were then used to calculate the mass flow rates discharged form the air reservoir by using the method proposed in our earlier study.[6] Herein, these calculated mass flow rates are treated as benchmark solutions and are validated to be accurate. Comparing the mass flow rate predicted by the proposed model with that of the benchmark solution reveals that the model prediction is about 10% overestimated. To obtain more accurate predictions, the process is more accurately simulated by considering the friction effects induced by the exit of the air reservoir and the nozzles on the blowpipe. The former increases the Mach number of the air and equals that of a frictional pipe of $4fLe/D_h$. The latter decreases the mass flow rate discharged from the nozzles. A discharge coefficient Cd_n is introduced to represent the ratio of the mass flow rate between a real nozzle and an ideal one. Also proposed herein are experimental methods to determine the values of $4fLe/D_h$ and Cd_n. Consequently, the accuracy of the model's predictions is significantly improved. Deviations between the mass flow rates of the model predictions and the benchmark solutions were within 3%. Furthermore, the pressure variations of the air in the reservoir and in the blowpipe of the model predictions agree well with those obtained from experimental work.

MODELING

Figure 1 illustrates the pulse-jet cleaning system, consisting primarily of an air reservoir, a diaphragm valve, and a blowpipe. On the blowpipe, a number of holes used as jet nozzles were drilled perpendicularly to the pipe. Each nozzle is located on the top of the filter bag coaxially.

Figure 2 schematically depicts the physical model. The air reservoir and the blowpipe are referred to as reservoir 1 and reservoir 2, respectively. The volume of reservoir 1 is V_{r1}, and the temperature, pressure, and mass of the air in reservoir 1 are $T_{r1,t}$, $P_{r1,t}$, and $m_{r1,t}$, respectively. The volume of reservoir 2 is V_{r2}, and the temperature, pressure, and mass of the air in reservoir 2 are $T_{r2,t}$, $P_{r2,t}$,

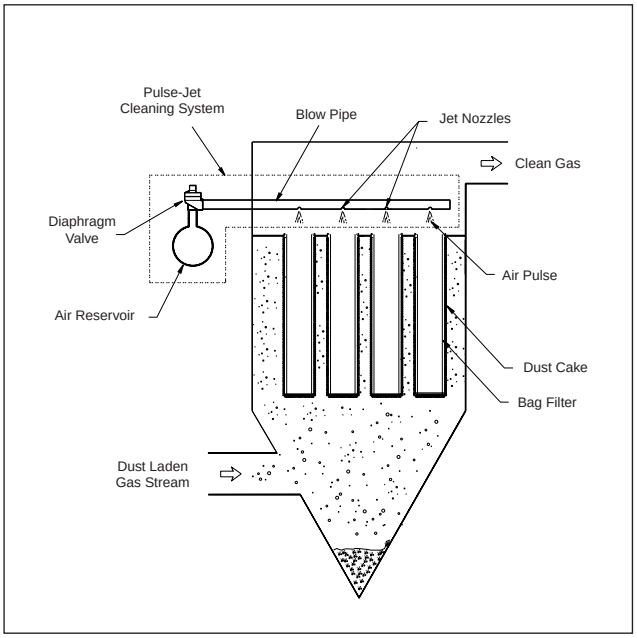

Figure 1. An illustration of a pulse-jet cleaning system.

and $m_{r2,t}$, respectively. Next, the subscripts u and d denote the properties of the air upstream and downstream of the diaphragm valve, respectively. The areas of the exits of reservoir 1 and reservoir 2 are equal to the cross-sectional area of the connecting pipe A_b and the total cross-sectional area of the nozzles on the blowpipe A_n, respectively. Finally, the mass flow rates discharged from reservoir 1 and reservoir 2 are $\dot{m}_{1,t}$ and $\dot{m}_{2,t}$, respectively.

The air discharging from reservoir 1 via reservoir 2 into the atmosphere takes a relatively short time. The process is regarded as adiabatic. In addition, the volume of the connecting pipe is much smaller than those of the reservoirs. The air properties along the connecting pipe are assumed to be the same as the diameters at the exit of reservoir 1. To facilitate the analysis, both the exits of reservoir 1 and reservoir 2 and the entrance of reservoir 2 are assumed to be frictionless. Consequently, the processes can be expressed reasonably with the following governing equations.

Initially, to differentiate the ideal-gas equation of state with respect to time t for the both reservoirs:

$$V_{r1}\frac{dP_{r1,t}}{dt} = m_{r1,t}R\frac{dT_{r1,t}}{dt} + RT_{r1,t}\frac{dm_{}}{d} \quad (1a)$$

$$V_{r2}\frac{dP_{r2,t}}{dt} = m_{r2,t}R\frac{dT_{r2,t}}{dt} + RT_{r2,t}\frac{dm_{r2}}{dt} \quad (1b)$$

where $\frac{dm_{r1,t}}{dt}$ and $\frac{dm_{r2,t}}{dt}$ denote the mass change rates of the air in reservoirs 1 and 2 at time t, respectively. Therefore

$$\frac{dm_{r1,t}}{dt} = -\dot{m}_{1,t} \quad (2a)$$

$$\frac{dm_{r2,t}}{dt} = \dot{m}_{1,t} - \dot{m}_{2,t} \quad (2b)$$

Assuming that the process is adiabatic, the internal energy change rates of the air in both reservoirs can be expressed as

$$\frac{d\left(m_{r1,t}e_{r1,t}\right)}{dt} = -\dot{m}_{1,t}h_{r1,t} \quad (3a)$$

$$\frac{d\left(m_{r2,t}e_{r2,t}\right)}{dt} = \dot{m}_{1,t}h_{r1,t} - \dot{m}_{2,t}h_{r2,t} \quad (3b)$$

where $de_{r1,t} = c_v dT_{r1,t}$, $h_{r1,t} = c_p T_{r1,t}$, and $\gamma = \frac{c_p}{c_v}$, then temperature change rates in both reservoirs can be derived as

$$\frac{dT_{r1,t}}{dt} = (1-\gamma)\frac{RT_{r1,t}^{\ 2}}{P_{r1,t}V_{r1}}\dot{m}_{1,t} \quad (4a)$$

$$\frac{dT_{r2,t}}{dt} = \frac{\gamma T_{r1,t}T_{r2,t} - T_{r2,t}^{\ 2}}{P_{r2,t}V_{r2}}\dot{m}_{1,t} + \frac{(1-}{1} \quad (4b)$$

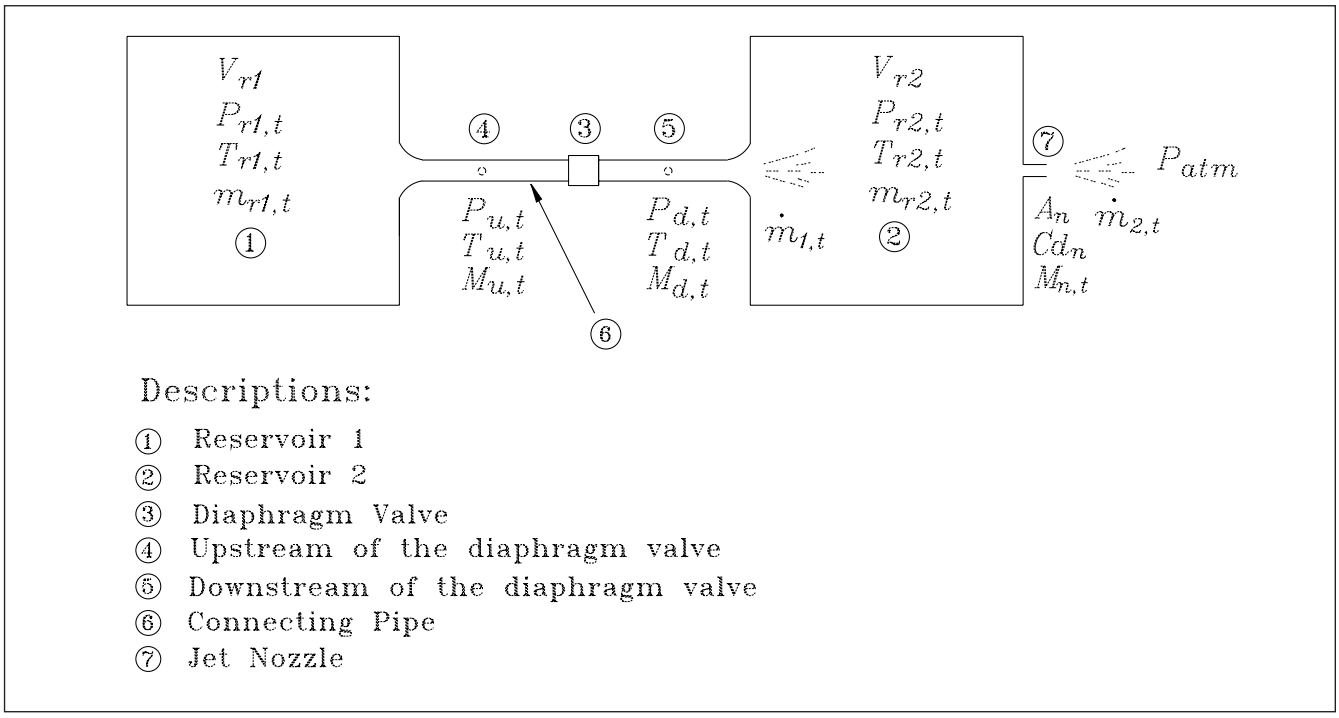

Figure 2. Physical model.

Substituting eq 4 into eq 1, the pressure change rates of the air in the reservoirs are expressed as

$$\frac{dP_{r1,t}}{dt} = -\frac{\gamma R T_{r1,t}}{V_{r1}} \dot{m}_{1,t} \tag{5a}$$

$$\frac{dP_{r2,t}}{dt} = \frac{\gamma R T_{r1,t}}{V_{r2}} \dot{m}_{1,t} - \frac{\gamma R T_{r2,t}}{V_{r2}} \dot{m}_{2,t} \tag{5b}$$

Notably, as shown in eqs 4 and 5, the pressure and temperature change rates of the air in both reservoirs are expressed in terms of $\dot{m}_{1,t}$ and $\dot{m}_{2,t}$.

According to Saad,[7] the mass flow rates $\dot{m}_{1,t}$ both upstream and downstream of the diaphragm valve may be expressed as

$$\dot{m}_{1,t} = \frac{P_{u0,t}}{\sqrt{T_{u0,t}}} \sqrt{\frac{\gamma}{R}} A_b \frac{M_{u,t}}{\left(1+\frac{\gamma-1}{2} M_{u,t}^{\ 2}\right)^{\frac{}{2(}}} \tag{6a}$$

$$\dot{m}_{1,t} = \frac{P_{d0,t}}{\sqrt{T_{d0,t}}} \sqrt{\frac{\gamma}{R}} A_b \frac{M_{d,t}}{\left(1+\frac{\gamma-1}{2} M_{d,t}^{\ 2}\right.} \tag{6b}$$

where the subscript *0* denotes the stagnation properties of the air. While assuming that the process is adiabatic and that the exit of reservoir 1 and the entrance of reservoir 2 are frictionless, both the stagnation temperatures of $T_{u0,t}$ and $T_{d0,t}$ are equal to $T_{r1,t}$ and the stagnation pressures of $P_{u0,t}$ and $P_{d0,t}$ are equal to $P_{r1,t}$ and $P_{r2,t}$, respectively. The static properties of $P_{u,t}$, $P_{d,t}$, $T_{u,t}$, and $T_{d,t}$ can be obtained from the following equations:[7]

$$P_{u,t} = P_{u0,t}\left(1+\frac{\gamma-1}{2} M_{u,t}^{\ 2}\right)^{\frac{\gamma}{1-\gamma}} \tag{7a}$$

$$P_{d,t} = P_{d0,t}\left(1+\frac{\gamma-1}{2} M_{d,t}^{\ 2}\right)^{\frac{\gamma}{1-\gamma}} \tag{7b}$$

and

$$T_{u,t} = \frac{T_{u0,t}}{1+\frac{\gamma-1}{2} M_{u,t}^{\ 2}} \tag{8a}$$

$$T_{d,t} = \frac{T_{d0,t}}{1+\frac{\gamma-1}{2} M_{d,t}^{\ 2}} \tag{8b}$$

Based on the results of our previous study,[6] the valve flow characteristics of the diaphragm valve can be expressed as

$$G_t = C_1 \ln(x_t) + C_2 \tag{9}$$

where C_1 and C_2 are empirical constants and the pressure ratio x_t and the dimensionless mass flow rate G_t are defined as

$$x_t = \frac{P_{u,t} - P_{d,t}}{P_{u,t}} \tag{10}$$

$$G_t = \frac{\dot{m}_{1,t}\sqrt{RT_{u,t}}}{A_b P_{u,t}} \tag{11}$$

Solving eqs 6–11, the variables $M_{u,t}$, $M_{d,t}$, $P_{u,t}$, $P_{d,t}$, $T_{u,t}$, $T_{d,t}$, x_t, G_t, and $\dot{m}_{1,t}$ are determined as the properties of $P_{r1,t}$, $P_{r2,t}$, $T_{r1,t}$, and $T_{r2,t}$.

The mass flow rate $\dot{m}_{2,t}$ discharged from reservoir 2 can be expressed as[7]

$$\dot{m}_{2,t} = \frac{P_{r2,t}}{\sqrt{T_{r2,t}}} \sqrt{\frac{\gamma}{R}} A_n \frac{M_{n,t}}{\left(1+\frac{\gamma-1}{2} M_{n,t}^{\ 2}\right)} \tag{12}$$

where $M_{n,t}$ denotes the Mach number of the air flow at the exit of the nozzle and can be solved by the following equation:

$$\frac{P_{r2,t}}{P_{atm}} = \left(1+\frac{\gamma-1}{2} M_{n,t}^{\ 2}\right)^{\frac{\gamma}{\gamma-1}} \tag{13}$$

Solving eqs 12 and 13, the variables $M_{n,t}$ and $\dot{m}_{2,t}$ are determined as the properties of $P_{r2,t}$, P_{atm}, and $T_{r2,t}$.

Therefore, both the mass flow rates of $\dot{m}_{1,t}$ and $\dot{m}_{2,t}$ are determined and are used to calculate the change rates of $\frac{dT_{r1,t}}{dt}$, $\frac{dT_{r2,t}}{dt}$, $\frac{dP_{r1,t}}{dt}$, and $\frac{dP_{r2,t}}{dt}$ from eqs 4 and 5. Then the properties of air in the both reservoirs at next time interval can be calculated by using the forward finite difference.

The calculation procedures for solving the above equations are summarized as follows:

(1) Obtain the initial air properties of $Pr_{1,t}$, $P_{r2,t}$, $T_{r1,t}$, and $T_{r2,t}$.
(2) Assume an initial mass flow rate $\dot{m}_{1,t}^{n=1}$, where the superscript *n* denotes the times of iteration.
(3) Let $P_{u0,t} = P_{r1,t}$ and $T_{u0,t} = T_{r1,t}$, then substitute *Pu0,t*, *Tu0,t*, and $\dot{m}_{1,t}^{n}$ into eq 6a and calculate the upstream Mach number $M_{u,t}^{n}$.

(4) Substitute $P_{u0,t}$ and $M_{u,t}^{n}$ into eq 7a and calculate the upstream static pressure $P_{u,t}^{n}$.
(5) Substitute $T_{u0,t}$ and $M_{u,t}^{n}$ into eq 8a and calculate the upstream static temperature $T_{u,t}^{n}$.
(6) Substitute $P_{u,t}^{n}$, $T_{u,t}^{n}$, and $\dot{m}_{1,t}^{n}$ into eq 11 and calculate the dimensionless mass flow rate G_t^{n}.
(7) Substitute G_t^{n} into eq 9 and calculate the pressure ratio x_t^{n}.
(8) Substitute $P_{u,t}^{n}$ and x_t^{n} into eq 10 and calculate the downstream static pressure $P_{d,t}^{n}$.
(9) Substitute $\dot{m}_{1,t}^{n}$ and $P_{d,t}^{n}$ into eqs 6b and 7b, respectively, and calculate the downstream stagnation pressure $P_{d0,t}^{n}$ and Mach number $M_{d,t}^{n}$.
(10) Adjust $\dot{m}_{1,t}^{n}$ to $\dot{m}_{1,t}^{n+1}$ and iterate from step 3 to step 9 until the conditions of $\left|M_{d,t}^{n=n+1}-1\right|<10^{-6}$ and $P_{d0,t}^{n}\geq P_{r2,t}$ or the conditions of $\left|\frac{\left(P_{d0,t}^{n+1}-P_{r2,t}\right)}{P_{r2,t}}\right|<10^{-6}$ and $M_{d,t}^{n}\leq 1$ are satisfied.
(11) Substitute $P_{r2,t}$ and P_{atm} into eq 13 and calculate the Mach number *Mn,t*.
(12) Substitute $P_{r2,t}$, $T_{r2,t}$, and *Mn,t* into eq 12 and obtain the mass flow rate $\dot{m}_{2,t}$.
(13) Substitute $Tr_{1,t}$, $T_{r2,t}$, $Pr_{1,t}$, $P_{r2,t}$, $\dot{m}_{1,t}^{n}$, and $\dot{m}_{2,t}$ into eqs 4 and 5 and obtain the temperature and pressure change rates of $\frac{dT_{r1,t}}{dt}$, $\frac{dT_{r2,t}}{dt}$, $\frac{dP_{r1,t}}{dt}$, and $\frac{dP_{r2,t}}{dt}$ for both reservoirs.
(14) Use the forward finite difference to obtain the properties of the air in the reservoirs at next time step $t+\Delta t$.

$$T_{r1,t+\Delta t}=T_{r1,t}+\frac{dT_{r1,t}}{dt}\Delta t \qquad (14a)$$

$$T_{r2,t+\Delta t}=T_{r2,t}+\frac{dT_{r2,t}}{dt}\Delta t \qquad (14b)$$

$$P_{r1,t+\Delta t}=P_{r1,t}+\frac{dP_{r1,t}}{dt}\Delta t \qquad (14c)$$

$$P_{r2,t+\Delta t}=P_{r2,t}+\frac{dP_{r2,t}}{dt}\Delta t \qquad (14d)$$

(15) Replace $P_{r1,t}$, $P_{r2,t}$, $T_{r1,t}$ and $T_{r2,t}$ by $P_{r1,t+\Delta t}$, $P_{r2,t+\Delta t}$, $T_{r1,t+\Delta t}$ and $T_{r2,t+\Delta t}$, respectively, in step 1;
(16) Iterate from step 2 to step 15 until the time of the diaphragm valve is closed. Meanwhile, the values of $\dot{m}_{1,t}$, $\frac{dP_{r1,t}}{dt}$ and $\frac{dT_{r1,t}}{dt}$ are zero; and
(17) Iterate from step 11 to step 15 until the pressure of $P_{r2,t}$ is equal to the atmospheric pressure P_{atm}.

EXPERIMENTAL APPARATUS AND PROCEDURE

Experiments were performed to examine the feasibility of the proposed model. Figure 3 illustrates the experimental apparatus. An air reservoir (1) with a volume of 0.1065 m^3 was used. The pressure $P_{r1,t}$ and temperature $T_{r1,t}$ of the air in the air reservoir were measured by the pressure transmitter (6) and the thermocouple (7), respectively. A connecting pipe (2) with a diameter of 43 mm and a length of 450 mm was used to connect the air reservoir and the diaphragm valve (3). The diaphragm valve had a nominal diameter of 1.5 in. Two pressure transmitters (6) were installed separately on both sides of the diaphragm valve to measure the pressure variations of $P_{u,t}$ and $P_{d,t}$ during the discharge process. Next, a blowpipe (4) with a length of 1750 mm and a diameter of 43 mm was connected at the downstream of the diaphragm valve. On the blowpipe, twelve nozzles (5) with a diameter of 8 mm were drilled perpendicularly to the blowpipe. Another pressure transmitter was installed at the end of the blowpipe to measure the stagnation pressure $P_{r2,t}$ of the air in the blowpipe. Finally, a programmable logic controller (PLC) (9) was used to generate the trigger for opening the diaphragm valve and starting the data acquisition unit (8).

Procedures of the experimental work were as follows:

(1) Measure and record the initial state pressure $P_{r1,t=i}$ and temperature $T_{r1,t=i}$ of the air in the air reservoir under a stable situation.
(2) Execute the PLC program to open the diaphragm valve under a designed duration *t* and start the data acquisition unit.
(3) Measure and record the pressure variations of $P_{r1,t}$, $P_{u,t}$, $P_{d,t}$, and $P_{r2,t}$.
(4) Measure and record the final state pressure $P_{r1,t=f}$ and temperature $T_{r1,t=f}$ of the air in the reservoir under a stable situation. The final state implies that the experimental work is completed and the values of $P_{r1,t}$ and $T_{r1,t}$ of the air in the reservoir are invariant.
(5) Change the test condition and repeat the above procedures until enough data are obtained.

Prior to conducting the experimental work, the pressure transmitters used were calibrated by a standard pressure gauge. These pressure transmitters are made of the TRANSBAR ceramic sensing element. The measuring range is 0–10 bar. The error is within 0.2% of full scale. The typical response time is less than 3 msec. These pressure transmitters are calibrated by a WIKA standard pressure gauge, which has a measuring range of 0–10 kg/cm^2, a scale division of 0.05 kg/cm^2, and accuracy

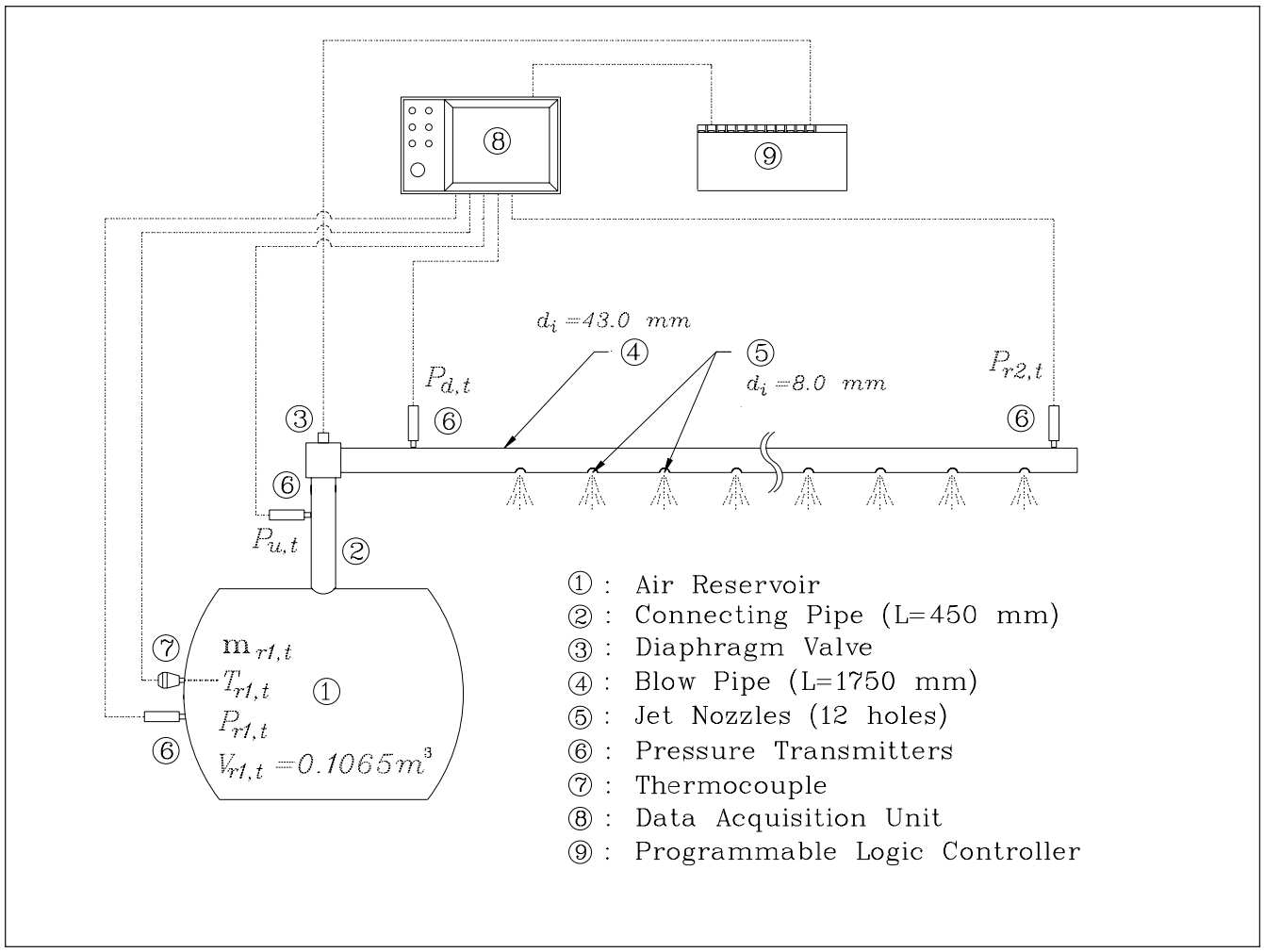

Figure 3. Experimental apparatus.

within 0.5% of full scale. Calibration results indicated that the discrepancies between the readings of the standard pressure gauge and those of the pressure transmitters were within 0.5%.

RESULTS AND DISCUSSION

Figure 4 presents the pressure variations during the discharge process. Figure 4a illustrates the pressure variations of $P_{r1,t}$ and $P_{u,t}$. Figure 4b illustrates the pressure variations of $P_{d,t}$ and $P_{r2,t}$. In this case, the duration of the electric pulse was 500 msec (from t = *400* msec to t = *900* msec). Due to the mechanical delay of the diaphragm valve, the beginning and the end of the variations of the pressures measured were slower than those of the electric pulse signals. These delays are estimated to be 30 msec and 150 msec, respectively.

After the diaphragm valve was opened, air was discharged from the air reservoir into the blowpipe. The discharged air decreased the pressures of $P_{r1,t}$ and $P_{u,t}$ and increases the pressures of $P_{d,t}$ and $P_{r2,t}$. After the pressure of $P_{r2,t}$ increased to a maximum value, all of the pressures of $P_{r1,t}$, $P_{u,t}$, $P_{d,t}$, and $P_{r2,t}$ monotonously decreased with time. At the moment the diaphragm valve was completely closed, the pressures of $P_{r1,t}$ and $P_{u,t}$ reached their minimums. After that, the pressures of $P_{r1,t}$ and $P_{u,t}$ gradually reached thermodynamic equilibrium. Meanwhile, the mass in the air reservoir $m_{r1,t}$ remained unchanged. The pressures of $P_{d,t}$ and $P_{r2,t}$ continuously decreased, however, until both pressures equaled the atmospheric pressure P_{atm}.

In the numerical calculations, the empirical constants C_1 and C_2 used in eq 9 are obtained from the results of our earlier study[6] and were equal to 0.1012 and 0.3933, respectively. The beginning of the discharge process was t = 430 msec, which equals the electric pulse turn-on time of t = 400 msec plus the diaphragm valve open delay time of 30 msec. The end of the discharge was t = 1050 msec, which equals the electric pulse turn-off time t = 900 msec plus the diaphragm valve close delay time 150 msec. Figure 4 indicates that the decreasing rates of $P_{r1,t}$ of the model prediction were greater than those of the experimental results. This phenomenon reveals that the prediction of the mass flow rate appears to be overestimated.

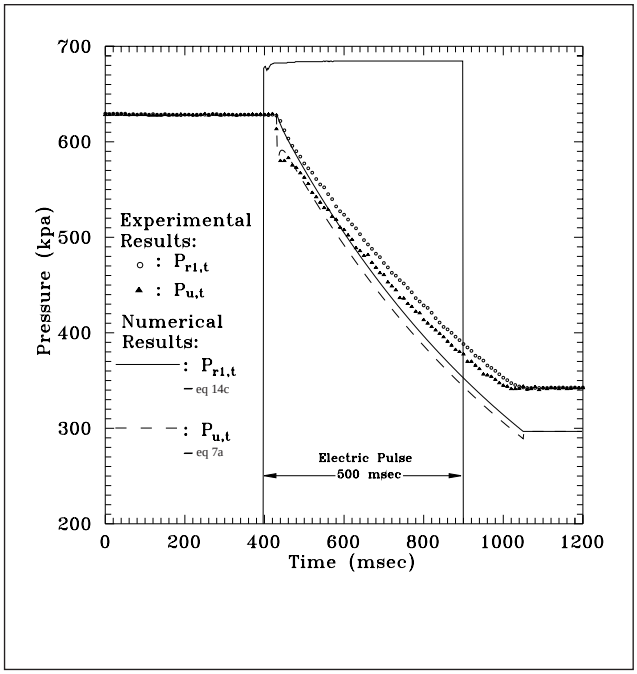

Figure 4(a). The pressure variations of $P_{r1,t}$ and $P_{u,t}$ under the condition of 12 jet nozzles.

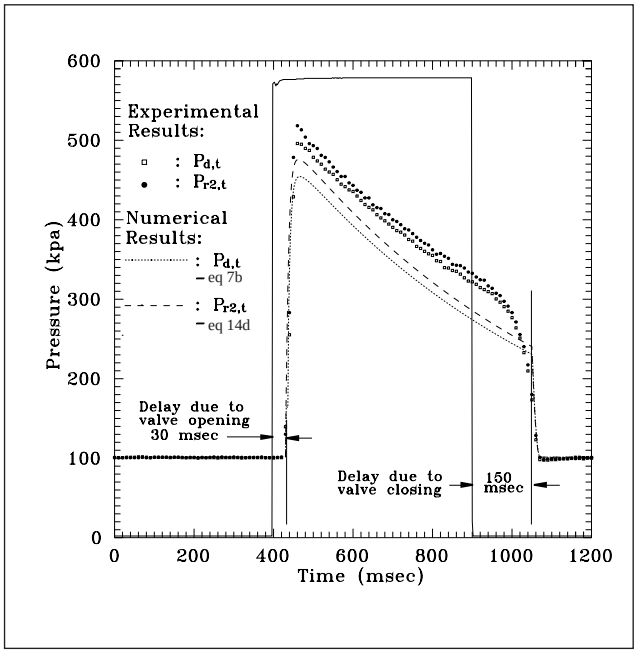

Figure 4(b). The pressure variations of $P_{d,t}$ and $P_{r2,t}$ under the condition of 12 jet nozzles.

Directly measuring the mass flow rate of a compressible transient process is extremely difficult. Therefore, to directly validate the accuracy of the mass flow rates predicted by the proposed model is impossible. According to our earlier study,[6] however, the residual mass $m_{r1,t}$ in the air reservoir and the mass flow rate $\dot{m}_{1,t}$ discharged from the air reservoir of an adiabatic process can be calculated from the pressure variation of $P_{r1,t}$ as

$$m_{r1,t} = m_{r1,t=i}\left(\frac{P_{r1,t}}{P_{r1,t=i}}\right)^{\frac{1}{\gamma}} \tag{15}$$

$$\dot{m}_{1,t} = -\frac{dm_{r1,t}}{dt} = -\frac{1}{\gamma}\frac{m_{r1,t=i}}{P_{r1,t}}\left(\frac{P_{r1,t}}{P_{r1,t=}}\right. \tag{16}$$

Figure 5 illustrates the results of $m_{r1,t}$ calculated from eq 15 by substituting the measured $P_{r1,t}$ shown in Figure 4 into the equation. In addition, Figure 5 also illustrates the residual mass $(m_{r1,t})_{iso}$ of an isothermal process to compare with the results from eq 15. The residual mass $(m_{r1,t})_{iso}$ is the lower limit of the realistic phenomena and can be calculated by the following equation:

$$\left(m_{r1,t}\right)_{iso} = m_{r1,t=i}\frac{P_{r1,t}}{P_{r1,t=i}} \tag{17}$$

According to Figure 5, the initial mass $m_{r1,t=i}$ and the final mass $m_{r1,t=f}$ are obtained by substituting the initial air properties ($P_{r1,t=i}$, $T_{r1,t=i}$) and the final air properties ($P_{r1,t=f}$, $T_{r1,t=f}$) into the ideal-gas equation of state. The final properties refer to a situation in which the experimental work is completed and the pressure and temperature of the air in the air reservoir are unchanged and can be accurately measured. Therefore, the difference between $mr_{1,t}$=*i* and

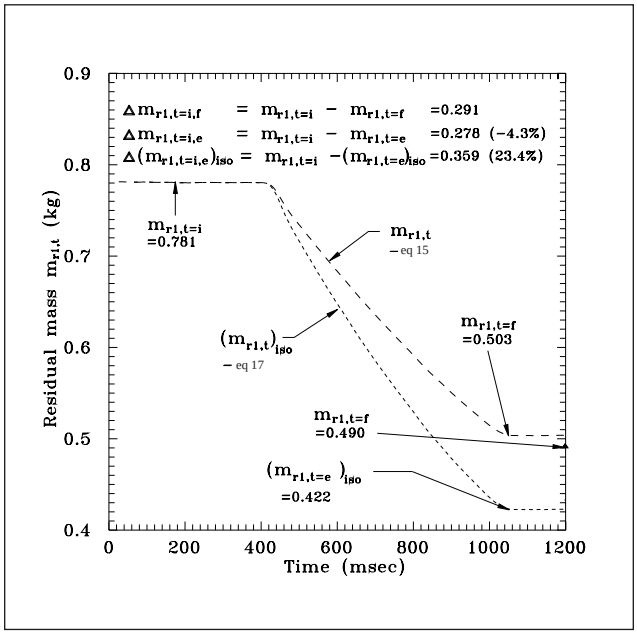

Figure 5. The variation of the residual mass of $m_{r1,t}$ under the condition of 12 jet nozzles.

Table 1. The comparisons of the cumulated mass discharged between the experimental results and those obtained from eq 15.

	(1)	(2)	(3)	(4)	(5)	(6)
	$m_{r1,t=i} = \frac{P_{r1,t=i}V_{r1}}{RT_{r1,t=i}}$	$m_{r1,t=e}$ $Eq.(15)$	$m_{r1,t=f} = \frac{P_{r1,t=f}V_{r1}}{RT_{r1,t=f}}$	$\Delta m_{r1,t=i,e} = m_{r1,t=i} - m_{r1,t=e}$	$\Delta m_{r1,t=i,f} = m_{r1,t=i} - m_{r1,t=f}$	Deviations $= \frac{\Delta m_{r1,t=i,e} - \Delta m_{r1,t=i,f}}{\Delta m_{r1,t=i,f}}$
Run No.	**(kg)**	**(kg)**	**(kg)**	**(kg)**	**(kg)**	**(%)**
1	0.7807	0.5029	0.4902	0.2779	0.2905	-4.35%
2	0.7957	0.4441	0.4343	0.3516	0.3614	-2.73%
3	0.7993	0.4441	0.4439	0.3445	0.3555	-3.08%
4	0.8283	0.4901	0.4783	0.3382	0.3500	-3.37%
5	0.8081	0.5052	0.4925	0.3029	0.3157	-4.04%
6	0.8158	0.5582	0.5466	0.2576	0.2692	-4.31%
7	0.7957	0.6132	0.6045	0.1825	0.1912	-4.59%
8	0.8116	0.6788	0.6721	0.1328	0.1395	-4.82%

$m_{r1,t=f}$ is 0.291 kg, which is reasonably regarded as the actual cumulated mass discharged $\Delta m_{r1,t=i,f}$ during the discharge process. The residual mass at the end of discharge of an adiabatic process and that at the end of an isothermal process—$m_{r1,t=e}$ and $(m_{r1,t=e})_{iso}$—are calculated by substituting the pressure $P_{r1,t=e}$ at the end of discharge into eq 15 and eq 17, respectively. By doing so, the cumulated mass discharged by an adiabatic process $\Delta m_{r1,t=i,e}$ and by an isothermal process $(\Delta m_{r1,t=i,e})_{iso}$ were obtained and were equal to 0.278 kg and 0.359 kg, respectively. Notably, the deviation between $\Delta m_{r1,t=i,e}$ and $\Delta m_{r1,t=i,f}$ was only 4.3%, which is much smaller than that between $\Delta m_{r1,t=i,e}$ and $(\Delta m_{r1,t=i,e})_{iso}$, which was 23.4%. Table 1 compares the cumulated mass discharge obtained from eq 15 and from experimental work under different operating conditions. All the deviations are smaller than 5%. From the above discussion, we can infer that the assumption that the process is adiabatic is adequate and that the results from eq 15 are accurate.

Because eq 16 is derived from eq 15, the mass flow rate $\dot{m}_{1,t}$ calculated from eq 16 is regarded to be accurate and is regarded as the benchmark solution for the numerical result obtained from the two-reservoir model proposed in this study. More extensive discussions on the accuracy of the mass flow rate calculated from eq 16 can be found in our previous study.[6]

Figure 6 illustrates the numerical results of the mass flow rate $\dot{m}_{1,t}$ and $\dot{m}_{2,t}$ obtained from the proposed model and the experimental results of the mass flow rate $\dot{m}_{1,t}$ calculated from eq 16. Apparently, the values of $\dot{m}_{1,t}$ and $\dot{m}_{2,t}$ in the numerical results are close to each other and are greater than the value of $\dot{m}_{1,t}$ of the experimental results. This finding implies that the mass flow rates predicted by the proposed model are overestimated. Except for the beginning and end of the discharge, the deviation between the mass flow rate $\dot{m}_{1,t}$ of the experimental results and the numerical results from $t = 500$ msec to $t = 900$ msec is about 10%. The deviations are more significant at the beginning and the end of the discharge. This is because although the diaphragm valve is assumed to be immediately fully opened or closed in model calculation, it is gradually opened or closed in an actual situation.

To obtain more accurate results, some modifications of the two-reservoir model are adopted. Herein, both the friction effects induced by the exit of the air reservoir and the nozzles of the blowpipe are considered. Initially, the friction effect induced by the exit of the air reservoir is represented by that of a frictional constant cross-sectional area pipe with a parameter of $\frac{4\bar{f}L_e}{D_h}$. According to Saad,[7] the relation between the Mach numbers of $M_{1,t}$ and $M_{2,t}$ at both sides of the frictional pipe can be expressed as

$$\frac{4\bar{f}L_e}{D_h} = \frac{1}{\gamma}\left(\frac{1}{M_{1,t}^2} - \frac{1}{M_{2,t}^2}\right) + \frac{\gamma+1}{2\gamma}\ln \cdot \tag{18}$$

The average friction coefficient $\bar{f}$ is defined as

$$\bar{f} = \frac{1}{L_e}\int_0^{L_e} f dx \tag{19}$$

Notably, the parameter of $\frac{4\bar{f}L_e}{D_h}$ is obtained in advance prior to use the proposed model. Various methods are available to determine the value of $\frac{4\bar{f}L_e}{D_h}$. Herein, a relatively simple method is proposed as an alternative to determine the parameter of $\frac{4\bar{f}L_e}{D_h}$. The method is described as follows.

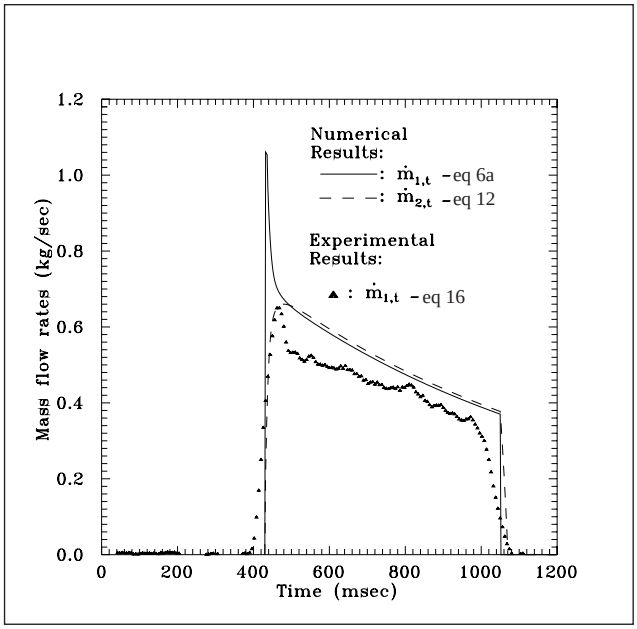

Figure 6. The variations of the mass flow rate of $\dot{m}_{1,t}$ and $\dot{m}_{2,t}$ under the condition of 12 jet nozzles.

Displacing the stagnation pressure $P_{u0,t}$ in eq 6a by $P_{r1,t}$ and substituting the mass flow rate $\dot{m}_{1,t}$ obtained from eq 16 into eq 6a allows us to calculate the Mach number $M_{1,t}$. On the other hand, the mass flow rate $\dot{m}_{1,t}$ can be expressed in terms of the static pressure of $P_{u,t}$ as[7]

$$\dot{m}_{1,t} = \frac{P_{u,t}}{\sqrt{T_{r1,t}}}\sqrt{\frac{\gamma}{R}}A_b M_{u,t}\sqrt{1+\frac{\gamma-1}{2}M_{\iota}} \qquad (20)$$

Substituting the measured static pressure $P_{u,t}$ measured and the mass flow rate $\dot{m}_{1,t}$ obtained from eq 16 into eq 20 allows us to obtain the Mach number $M_{u,t}$, which is regarded as $M_{2,t}$ in eq 18. Finally, substituting the determined Mach numbers $M_{1,t}$ and $M_{2,t}$ into eq 18 allows us to calculate the parameter of $\frac{4\bar{f}L_e}{D_h}$.

Figure 7 illustrates the Mach numbers $M_{1,t}$ and $M_{2,t}$ and the parameter $\frac{4\bar{f}L_e}{D_h}$. Except for the beginning and end of the discharge, the time average value of $\frac{4\bar{f}L_e}{D_h}$ from t = *500* msec to t = *900* msec is about 0.74.

As for the nozzles on the blowpipe, the friction effect resulted in a mass flow rate discharged from an actual nozzle that was lower than that discharged from an ideal nozzle. Therefore the real mass flow rate $\dot{m}_{2,t}$ discharged from the blowpipe can be expressed by introducing the discharge coefficient Cd_n into eq 12 as

$$\dot{m}_{2,t} = \frac{P_{r2,t}}{\sqrt{T_{r2,t}}}\sqrt{\frac{\gamma}{R}}A_n Cd_n \frac{M_n}{\left(1+\frac{\gamma-1}{2}M\right.} \qquad (21)$$

In the model calculations, the value of Cd_n must also be known in advance. The value of Cd_n is usually determined according to the standard test procedure of ANSI/ASME[8]. Herein, an alternative is proposed to determine the value of Cd_n by using the measured pressure variations shown in Figure 4. In addition to the fact that the volume of the blowpipe is markedly smaller than that of the air reservoir, the discharge process is extremely rapid and the value of $\dot{m}_{1,t}$ is close to the value of $\dot{m}_{2,t}$ at the same time t. Therefore the value of $T_{r2,t}$ is considered to be equal to the value of $Tr_{1,t}$. In addition, the time-dependent temperature $T_{r1,t}$ can be calculated by the following equation:

$$T_{r1,t} = T_{r1,t=i}\left(\frac{P_{r1,t}}{P_{r1,t=i}}\right)^{\frac{\gamma-1}{\gamma}} \qquad (22)$$

Therefore the mass flow rate $\left(\dot{m}_{2,t}\right)_{isen}$ of an insentropic flow can be determined by substituting the stagnation temperature $T_{r2,t\,(=Tr1,t)}$ and the measured pressure $P_{r2,t}$ into eq 12. Then the discharge coefficient Cd_n can be determined by the following equation:

$$Cd_n = \frac{\left(\dot{m}_{2,t}\right)_{real}}{\left(\dot{m}_{2,t}\right)_{isen}} \approx \frac{\dot{m}}{\frac{P_{r2,t}}{\sqrt{T_{r1,t}}}\sqrt{\frac{\gamma}{R}}\frac{}{\left(1+\right.}} \qquad (23)$$

Where the Mach number $M_{n,t}$ is calculated by substituting the measured pressure $P_{r2,t}$ into eq 13.

Figure 8 plots the results of $\left(\dot{m}_{2,t}\right)_{real}$ from eq 16, $\left(\dot{m}_{2,t}\right)_{isen}$ from eq 12, and C_{dn} obtained from eq 23.

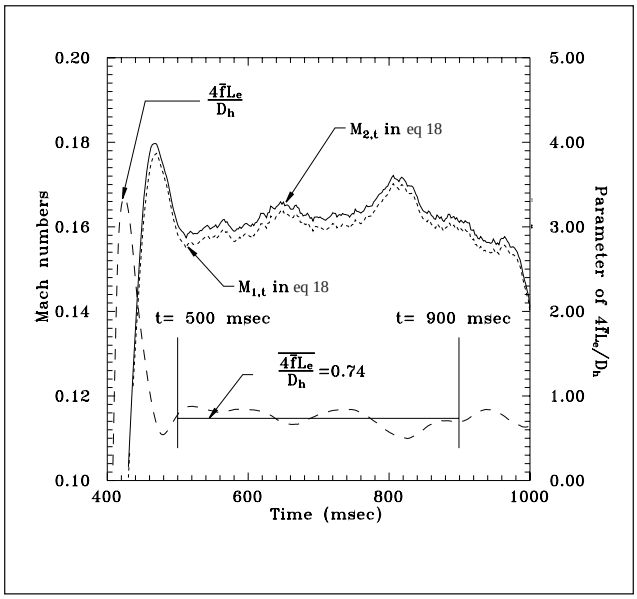

Figure 7. The variations of the Mach number of $M_{u,t}$ and the parameter of $\frac{4\bar{f}L_e}{D_h}$ under the condition of 12 jet nozzles.

Except for the beginning and end of the discharge, the average value of Cd_n from $t = 500$ msec to $t = 900$ msec is about 0.78.

As the parameters of $\frac{4\bar{f}L_e}{D_h}$ and Cd_n are adopted into the model, some of the calculation procedures must be modified as follows.

(a) Divide step 3 in the above calculation procedure into three parts: 3-1, 3-2, and 3-3.
  (3-1) Displace $P_{u0,t}$ and $T_{u0,t}$ by $P_{r1,t}$ and $T_{r1,t}$ in eq 6a, respectively. And then the Mach number $M^n_{u,t}$ is calculated and regarded as $M^n_{1,t}$ in eq 18.
  (3-2) Substitute the values of $\frac{4\bar{f}L_e}{D_h}$ (= 0.74) and $M^n_{1,t}$ into eq 18 to obtain the Mach number $M^n_{2,t}$.
  (3-3) Displace $M^n_{u,t}$ by $M^n_{2,t}$ in eq 6a and obtain the value of $P^n_{u0,t}$.

(b) Renew step 4. Substitute $P^n_{u0,t}$ and $M^n_{u,t}$ into eq 7a and calculate the upstream static pressure $P^n_{u,t}$.

(c) Renew step 12. Substitute $P_{r2,t}$, $T_{r2,t}$, and Mn,t into eq 21. In doing so, the mass flow rate of $\dot{m}_{2,t}$ is obtained.

Figure 9 illustrates the variations of pressures and the mass flow rates of the model predictions and the experimental results. In model calculation, the values of $\frac{4\bar{f}L_e}{D_h}$ and Cd_n are equal to 0.74 and 0.781, respectively. Experimental results are the same as those shown in Figures 4 and 6. Figure 9 indicates that all of the pressures and mass flow rates of the model predictions agree well with the experimental results. The deviation between the average mass flow rate of $\dot{m}_{r1,t}$ from $t = 500$ msec to $t = 900$ msec of the model predictions and the bench mark solutions is about 0.61%.

For validating the proposed model, some of the nozzles on the blowpipe are blocked to change the total discharge area A_n of the blowpipe. Figure 10 summarizes the results of the variations of the pressures and of the mass flow rates, which are obtained under the condition of eight nozzles being opened and four nozzles being blocked. The values of Cd_n and $\frac{4\bar{f}L_e}{D_h}$ employed in the model are the same as those used in the previous case. According to Figure 10, the variations of the pressures and the mass flow rates of the numerical results well with the experimental results. The deviation between the average mass flow rate of $\dot{m}_{r1,t}$ from $t = 500$ msec to $t = 900$ msec of the model predictions and the bench mark solutions is about 0.85%. Table 2 compares the average mass flow rates under different discharge areas. The maximum deviation between the numerical and experimental results is smaller than 3%. Obviously, considering the friction effects of the exits of both reservoirs significantly improves the accuracy of the model predictions.

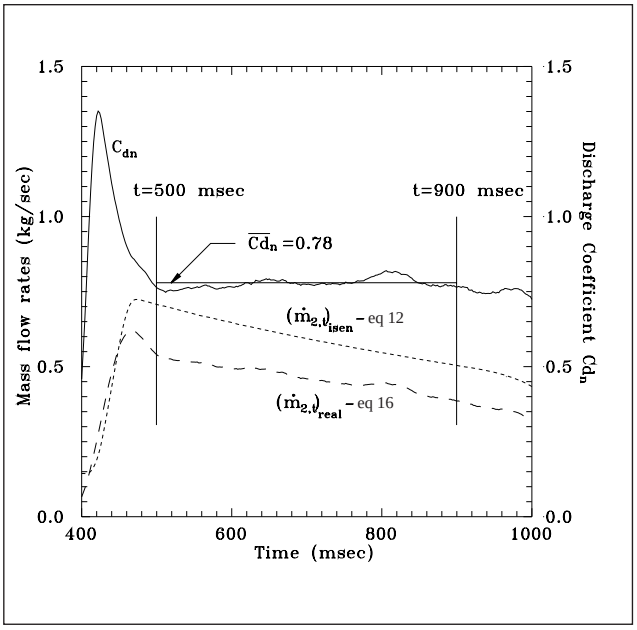

Figure 8. The variations of the mass flow rate of $\dot{m}_{1,t}$ and $\dot{m}_{2,t}$ and the discharge coefficient Cd_n under the condition of 12 jet nozzles.

CONCLUSION

This study presents a novel two-reservoir model to simulate the air discharged from an air reservoir via a diaphragm valve to a blowpipe and ultimately into the atmosphere of a pulse-jet cleaning system. Based on the results in this study, we can conclude the following:

(1) Without considering the friction effects of the exits of both reservoirs, the mass flow rates of the model predictions are about 10% overestimated.

(2) Introducing a parameter of $4fLe/D_h$ and a discharge coefficient Cd_n into the governing equations allowed us to successfully simulate the friction effects induced by the exit of the air reservoir and the nozzles on the blowpipe. The experimental methods to determine both $4fLe/D_h$ and Cd_n are also presented.

(3) The proposed model is more accurately simulated by considering the friction effects induced by the exit of the air reservoir and the nozzles on the blowpipe. The accuracy is significantly improved. Deviations between the mass flow rates of the model predictions with those of the bench mark solutions are smaller than 3%. Moreover, the pressure variations of the model predictions agree well with those obtained by experimental work.

ACKNOWLEDGMENT

The authors would like to thank the National Science Council of the Republic of China and the Taiwan Power Company for financially supporting this research under Contract No. NSC-87-TPE-E-009-007.

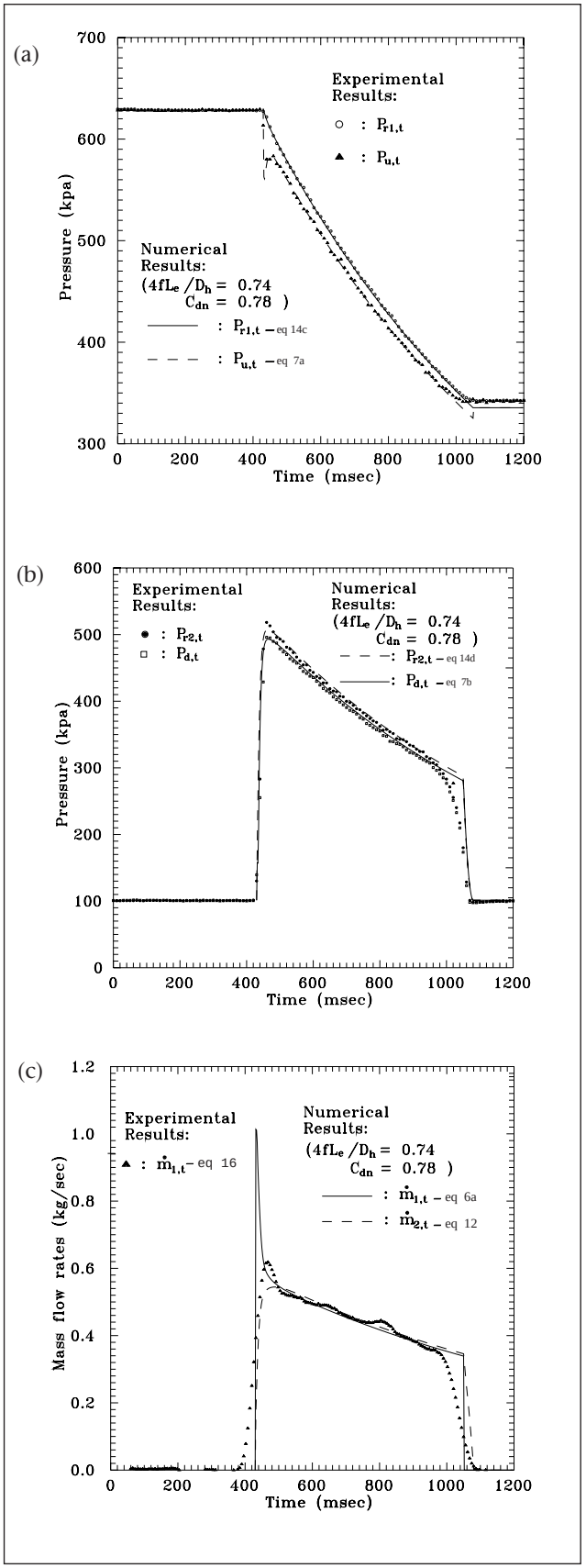

Figure 9. (a)The pressure variations of $P_{r1,t}$ and $P_{u,t}$ under the condition of 12 nozzles. (b). The pressure variations of $P_{d,t}$ and $P_{r2,t}$ under the condition of 12 nozzles. (c). The variations of the mass flow rate of $\dot{m}_{1,t}$ and $\dot{m}_{2,t}$ under the condition of 12 nozzles.

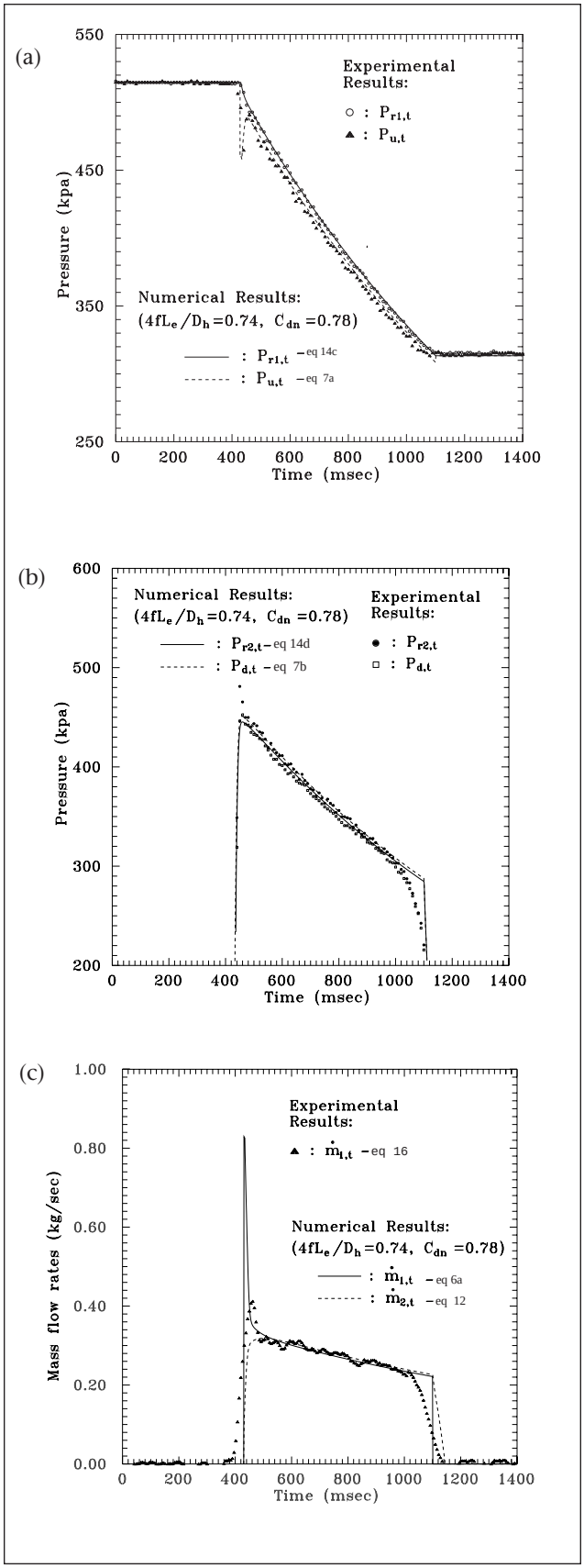

Figure 10. (a) The pressure variations of $P_{r1,t}$ and $P_{u,t}$ under the condition of 8 nozzles. (b) The pressure variations of $P_{d,t}$ and $P_{r2,t}$ under the condition of 8 nozzles. (c) The variations of the mass flow rate of $\dot{m}_{1,t}$ and $\dot{m}_{2,t}$ under the condition of 8 nozzles.

Table 2. The comparisons of the average mass flow rates between the experimantal results and the numerical results.

Experimental Conditions		Average Mass Flow Rate from t=500 msec to t=900 msec				
Initial Pressure $P_{r1,t=I}$ (kpa)	Initial Temperature $T_{r1,t=I}$ (K)	Jet Nozzles Opened/Blocked	Experimental Results eq 16 (kg/sec)	Numerical Results $4fL_e/D_h=0.74$ $Cd_n=0.78$ (kg/sec)	Deviations (%)	Remark
629.7	293.7	12 / 0	0.4602	.04574	-0.67%	Fig. 9c
515.8	298.8	12 / 0	0.3755	0.3744	-0.29%	
514.5	299.1	8 / 4	0.2859	0.2835	-0.85%	Fig. 10c
512.8	299.0	4 / 8	0.1624	0.1596	-1.74%	
517.1	299.1	2 / 10	0.0894	0.0867	-2.99%	
517.9	299.4	1 / 11	0.0469	0.0458	-2.31%	

NOMENCLATURE

Ab = blowpipe cross-sectional area, m^2
An = total cross-sectional area of the nozzles on the blowpipe, m^2
Cp = constant-pressure specific heat, kJ/(kg K)
Cv = constant-volume specific heat, kJ/(kg K)
C_1, C_2 = constant
Cd_n = discharge coefficient of the nozzle, ratio of the real mass flow rate to the mass flow rate of an isentropic flow, $=\frac{(\dot{m})_{real}}{(\dot{m})_{isen}}$, dimensionless
d = diameter, m
D_h = hydraulic diameter, m
e = specific internal energy of air in a reservoir, kJ/kg
f = friction factor, dimensionless
G = dimensionless mass flow rate, defined by eq 11, dimensionless
h = specific enthalpy of air in a reservior, kJ/kg
m = mass of air in a reservior, (= *PV/RT*), kg
Δm = cumulated mass discharged, kg
$\dot{m}$ = mass flow rate discharged from flow reservoir, kg/sec
M = Mach number, dimensionless
P*atm* = atmospheric pressure, kPa
P = absolute pressure, kPa
R = gas constant of air, (=*287.04*), $m^2/(s^2\ K)$
T = temperature, K
V = volume, m^3
x = ratio of pressure drop to absolute upstream pressure, $(=(P_u-P_d)/P_u)$, dimensionless
= ratio of specific heats, (=*Cp/Cv*), dimensionless

Subscripts

0 = stagnation properties
r1 = the reservoir 1, (the air reservoir)
r2 = the reservoir 2, (the blowpipe)
u = the upstream of the diaphragm valve
d = the downstream of the diaphragm valve
i = the initial state
e = at the end of discharge
f = the final state
t = time

Superscript

n = times of iteration

REFERENCES

1. Morris, W.J. "Cleaning mechanisms in pulse jet fabric filters," *Filtration & Separation* **1984**, *21*, 50-54.
2. Bouilliez, L. "Importance of physical parameters for the cleaning efficiency of a reverse jet-cleaned dust collector," Solids Handling Conference, Harrogater, England, 1986, pp B11-B25.
3. Sievert, J.; Löffler, F. "The effect of cleaning system parameters on the pressure pulse in a pulse-jet filter," *Particulate and Multiphase Processes Conference*, Miami, FL, 1987; Vol.2, pp 647-662.
4. De Ravin, M.; Humphries; W.; and Postle, R. "A model for the performance of a pulse jet filter," *Filtration & Separation* **1988**, *25*, 201-207.
5. Hajek, S.; Peukert, W. "Experimental investigations with ceramic high-temperature filter media," *Filtration & Separation* **1996**, *33*, 29-37.
6. Fu, W.S.; Ger, J.S. "A concise method for determining a valve flow coefficient of a valve under compressible gas flow," *Experimental Thermal & Fluid Sci*., in press.
7. Saad, M.A. *Compressible Fluid Flow*; 2nd ed.; Prentice Hall: New Jersey, 1993; Chapter 3.
8. *Performance Test Cords on Safety and Relief Valves*; The American Society of Mechanical Engineers: New York, 1976; ANSI/ASME PTC 25.3-19.

About the Authors

Dr. W.S. Fu is a professor in the Mechanical Engineering Department of Chiao Tung University, Hsinchu, 30050, Taiwan, R.O.C. J. S. Ger is a Ph.D. student in the Mechanical Engineering Department of Chiao Tung University and a researcher in the Energy & Resources Laboratories of Industrial Technology Research Institute. Correspondence should be sent to Dr. W.S. Fu, Professor, Mechanical Engineering Department, Chiao Tung University, 1001 Ta Hsueh Rd., Hsinchu, 30050, Taiwan, R.O.C.